

The trispectrum of 21-cm background anisotropies as a probe of primordial non-Gaussianity

Asantha Cooray¹, Chao Li², Alessandro Melchiorri³

¹*Center for Cosmology, Department of Physics and Astronomy,
4129 Frederick Reines Hall, University of California, Irvine, CA 92697*

²*Theoretical Astrophysics, California Institute of Technology, Mail Code 103-33 Pasadena, California 91125*

³*Dipartimento di Fisica “G. Marconi” and INFN, sezione di Roma,
Universita’ di Roma “La Sapienza”, Ple Aldo Moro 5, 00185, Roma, Italy.*

(Dated: October 26, 2018)

The 21-cm anisotropies from the neutral hydrogen distribution prior to the era of reionization is a sensitive probe of primordial non-Gaussianity. Unlike the case with cosmic microwave background, 21-cm anisotropies provide multi-redshift information with frequency selection and is not damped at arcminute angular scales. We discuss the angular trispectrum of the 21-cm background anisotropies and discuss how the trispectrum signal generated by the primordial non-Gaussianity can be measured with the three-to-one correlator and the corresponding angular power spectrum. We also discuss the separation of primordial non-Gaussian information in the trispectrum with that generated by the subsequent non-linear gravitational evolution of the density field. While with the angular bispectrum of 21-cm anisotropies one can limit the second order corrections to the primordial fluctuations below $f_{\text{NL}} \sim 1$, using the trispectrum information we suggest that the third order coupling term, f_2 or g_{NL} , can be constrained to be around 10 with future 21-cm observations over the redshift interval of 50 to 100.

PACS numbers: 98.80.Es,95.85.Nv,98.35.Ce,98.70.Vc

I. INTRODUCTION

The cosmic 21-cm background involving spin-flip line emission or absorption of neutral hydrogen contains unique signatures on how the neutral gas evolved from last scattering at $z \sim 1100$ to complete reionization at $z < 10$ [1]. Subsequent to recombination, the temperature of neutral gas is coupled to that of the cosmic microwave background (CMB). At redshifts below ~ 200 the gas cools adiabatically, its temperature drops below that of the CMB, and neutral hydrogen resonantly absorbs CMB flux through the spin-flip transition [2, 3, 4]. The inhomogeneous neutral hydrogen density distribution generates anisotropies in the brightness temperature measured relative to the blackbody CMB [5]. The large cosmological and astrophysical information content in 21-cm background is well understood in the literature [3, 6, 7, 8, 9, 10, 11].

Parallel to the large effort in analytical and numerical calculations of the 21-cm properties, there are now several first generation 21-cm experiments underway focusing on the 21-cm signal during the era of reionization. At the low redshifts probed by these first generation interferometers, the 21-cm signal is modified by the astrophysics of first sources and the associated UV photon background. There, one naturally expects fluctuations to be dominated by inhomogeneities in source properties [12, 13]. The associated non-Gaussianity in 21-cm anisotropies leads to a measurable three-point correlation function or a bispectrum [14, 15, 16]. Such a non-Gaussianity is also expected to dominate the signature in 21-cm anisotropies generated by the primordial non-Gaussian density field. However, the 21-cm background generated by neutral hydrogen at redshifts of 50 to 100 prior to the onset of reionization and the appearance of first stars is expected to provide a cleaner probe of the primordial density perturbations in the same manner CMB observations are used to study primordial fluctuations [3]. If the primordial fluctuations are non-Gaussian, then the 21-cm anisotropies at these high redshifts will naturally contain a signature associated with that non-Gaussianity [17, 18]

The primordial non-Gaussianity in the density field can be studied with the three-point and higher-order correlation functions of the 21-cm background. In particular, the second order corrections to the density perturbations generated by primordial non-Gaussianity lead to a bispectrum with a dependence on the second-order correction to the curvature perturbations, f_{NL} [19, 22]. With future low frequency data out to $z \sim 100$, 21-cm background anisotropies could potentially limit $f_{\text{NL}} < 0.1$ [17]. In comparison, the expected non-Gaussianity under standard inflation is of order $|n_s - 1|$ and with the scalar spectral index $n_s \sim 0.98$ [29], f_{NL} is expected to be well below unity [25]. The primordial non-Gaussianity parameter at the second order f_{NL} , however, has a correction associated with evolution of second and higher-order perturbations after inflation [26]. For standard slow-roll inflation then $f_{\text{NL}} = -5/12(n_s - 1) + 5/6 + 3/10f(k)$ where the last term is momentum dependent. In this case f_{NL} is at the level of a few tenths and could be as high as 1. The ability for 21-cm anisotropies to probe f_{NL} as low as 0.1 is important since even a perfect CMB experiment limited by cosmic variance alone can only restrict $f_{\text{NL}} > 3$ [19, 20, 21] while there is no significant

improvement when using low redshift large-scale structure [23, 24].

The possibility to make primordial non-Gaussianity measurements with the 21-cm background is important since compared to most other probes of inflationary parameters, f_{NL} is one of the few parameters for which we have limited number of probes sensitive to the low amplitude non-Gaussianity expected under standard slow-roll inflation. While CMB as a probe of non-Gaussianity is well known, when compared to CMB temperature and polarization anisotropies, 21-cm background has two distinct advantages: (1) the ability to probe multiple redshifts based on frequency selection and (2) the lack of a damping tail in the 21-cm anisotropy spectrum, unlike damping of CMB anisotropies at a multipole around 2000.

While the 21-cm background as a potentially interesting and a useful probe of f_{NL} is now known, different scenarios for primordial fluctuations may produce a small f_{NL} but a large third-order correction. In certain alternative models of inflation higher order terms may be significant even if the second-order term is small and such scenarios include the new ekpyrotic cosmology [27] and, under certain conditions, the curvaton model [28]. Thus, beyond the non-Gaussianity at the three-point level with the bispectrum, it is also useful to study the non-Gaussianities of the 21-cm background at the four point-level involving the trispectrum.

Here we show that the angular trispectrum of 21-cm anisotropies contains a measurable non-Gaussianity from primordial fluctuations if the scale-independent cubic corrections to the gravitational potential captured with an amplitude parameter f_2 (or g_{NL} as described in Ref. [30]) has a value of order ~ 10 , even if the scale-independent quadratic corrections to the gravitational potential captured by f_{NL} has a value around ~ 1 . While f_{NL} is currently constrained with WMAP data [29], there is no real constraint on this third order non-Gaussianity parameter. There are, however, theoretical expectations: for slow-roll inflation, a trispectrum of the form $T_4 = 1/2\tau_{\text{NL}}[P(k_1)P(k_2)P(k_3) + \dots]$ is expected for curvature perturbations [31] with an expectation value of $\tau \lesssim r/50$ where r is the tensor-to-scalar ratio ($r \lesssim 0.6$ is recent CMB data [29]). In such a model, there is also a direct connection between τ_{NL} and f_{NL} such that $\tau_{\text{NL}} = (6f_{\text{NL}}/5)^2$ (see the discussion in Ref. [32] for connections between coupling terms of various models for primordial trispectrum). While such a relation is generally assumed when constraining τ_{NL} [33], in future it may be that one can directly test the above relation between f_{NL} and τ_{NL} with data.

To measure the non-Gaussianity at the four-point level, we introduce the three-to-one correlator statistic, extending the two-to-one correlator of Ref. [34] and applied to WMAP data in Ref. [35]. We optimize the angular power spectrum of the 3-1 correlator to detect the primordial trispectrum by appropriately filtering 21-cm anisotropy data to remove the non-Gaussian confusion generated by the non-linear evolution of gravitational perturbations. To do this properly, one requires prior knowledge on the configuration dependence of the primordial 21-cm trispectrum, but its amplitude is a free variable to be determined from the data.

This paper is organized as following: we first discuss the bispectrum in 21-cm anisotropies associated with primordial perturbations resulting from quadratic corrections to the primordial potential. We discuss ways to measure this bispectrum in the presence of other non-Gaussian signals and determine the extent to which f_{NL} can be measured from 21-cm background data. In the numerical calculations described later, we take a fiducial flat- Λ CDM cosmological model with $\Omega_b = 0.0418$, $\Omega_m = 0.24$, $h = 0.73$, $\tau = 0.092$, $n_s = 0.958$, and $A(k_0 = 0.05 \text{ Mpc}^{-1}) = 2.3 \times 10^{-9}$. This model is consistent with recent measurements from WMAP [29].

II. CALCULATIONAL METHOD

The 21-cm anisotropies are observed as a change in the intensity of the CMB due to line emission or absorption at an observed frequency ν :

$$T_b(\hat{\mathbf{n}}, \nu) = \frac{T_S - T_{\text{CMB}}}{1+z} \tau(\hat{\mathbf{n}}, \nu) \quad (1)$$

where T_S is the spin temperature of the neutral gas, z is the redshift corresponding to the frequency of observation ($1+z = \nu_{21}/\nu$, with $\nu_{21} = 1420 \text{ MHz}$) and $T_{\text{CMB}} = 2.73(1+z)K$ is the CMB temperature at redshift z . The optical depth, τ , in the hyperfine transition [2], when accounted for density and velocity perturbations of a patch in the neutral hydrogen distribution [3, 4, 5], is

$$\tau = \frac{3c^3 \hbar A_{10} \bar{n}_{\text{H}}}{16k_B \nu_{21}^2 T_S H(z)} \left(1 + \delta_H - \frac{1+z}{H(z)} \frac{\partial v}{\partial r} \right), \quad (2)$$

where A_{10} is the spontaneous emission coefficient for the transition ($2.85 \times 10^{-15} \text{ s}^{-1}$), n_{HI} is the neutral hydrogen density, $\delta_H = (n_{\text{H}} - \bar{n}_{\text{H}})/\bar{n}_{\text{H}}$ is the inhomogeneity in the density, v is the peculiar velocity of the neutral gas distribution, r is the comoving radial distance, and $H(z)$ is the expansion rate at a redshift of z . For simplicity, we have dropped

the dependences in location $\hat{\mathbf{n}}$. The fluctuations in the CMB brightness temperature is

$$\delta T_b = \bar{T}_b \left[\left(1 - \frac{T_{\text{CMB}}}{\bar{T}_S} \right) \left(\delta_H - \frac{1+z}{H(z)} \frac{\partial v}{\partial r} \right) + \frac{T_{\text{CMB}}}{\bar{T}_S} S \delta_H \right], \quad (3)$$

where $S(z)$ describes the coupling between fluctuations in the spin temperature and the neutral density distribution [4], δ_H is fluctuations in the neutral density distribution, and $v(r)$ is the peculiar velocity. In above $\bar{T}_b \approx 26.7 \text{mK} \sqrt{1+z}$ [5].

We describe fluctuations in the 21-cm background in terms of multiple moments defined as $a_{lm}(\nu) = \int d\hat{\mathbf{n}} Y_{lm}^*(\hat{\mathbf{n}}) \delta T_b(\hat{\mathbf{n}}, \nu)$ where

$$\begin{aligned} a_{lm}(\nu) &= \int d\hat{\mathbf{n}} Y_{lm}^*(\hat{\mathbf{n}}) \int dr W_\nu(r) \bar{T}_b(r) \left[\left(1 - \frac{T_{\text{CMB}}}{\bar{T}_S} \right) \left(\delta_H - \frac{1+z}{H(z)} \frac{\partial v}{\partial r} \right) + \frac{T_{\text{CMB}}}{\bar{T}_S} S \delta_H \right] \int \frac{d^3 \mathbf{k}}{(2\pi)^3} \delta_H(\mathbf{k}, r) e^{-i\mathbf{k} \cdot \hat{\mathbf{n}} r} \\ &= 4\pi (-i)^l \int dr W_\nu(r) \int \frac{d^3 \mathbf{k}}{(2\pi)^3} f_k(r) M(k) D(r) \Phi^{\text{prim}}(\mathbf{k}) Y_{lm}^*(\hat{\mathbf{k}}). \end{aligned} \quad (4)$$

In above,

$$f_k(r) = \bar{T}_b(r) \left[\left(1 - \frac{T_{\text{CMB}}}{\bar{T}_S} \right) J_l(kr) + \frac{T_{\text{CMB}}}{\bar{T}_S} S j_l(kr) \right], \quad (5)$$

with $J_l(x) = j_l(x) - j_l''(x)$. In equation (4), $D(r)$ is the growth function of density perturbations, $M(k) = -3k^2 T(k)/5\Omega_m H_0^2$ maps the primordial potential fluctuations to that of the density field.

For simplicity in notation, hereafter, we will drop the explicit dependence on the frequency, but it should be assumed that 21-cm background measurements can be constructed as a function of frequency, and thus as a function of redshift, with the width in frequency space primarily limited by the bandwidth of a radio interferometer captured by the window function $W_\nu(r)$.

Similar to calculations related to the CMB anisotropies, we can introduce a transfer function and rewrite multipole moments of 21-cm anisotropies as

$$a_{lm} = 4\pi (-i)^l \int \frac{d^3 \mathbf{k}}{(2\pi)^3} \Phi^{\text{prim}}(\mathbf{k}) g_{21\text{cm},l}(k) Y_{lm}^*(\hat{\mathbf{k}}), \quad (6)$$

with the transfer function of the 21-cm background anisotropies given by

$$g_{21\text{cm},l}(k) = \left[\int dr W_\nu(r) f_k(r) D(r) \right] M(k). \quad (7)$$

For reference, the angular power spectrum of 21-cm anisotropies follows by taking $\langle a_{lm} a_{l'm'}^* \rangle = C_l \delta_{ll'} \delta_{mm'}$ as

$$C_l(\nu) = \frac{2}{\pi} \int k^2 dk P_{\Phi\Phi}(k) g_{21\text{cm},l}^2(k), \quad (8)$$

where the power spectrum of Newtonian potential is defined such that $\langle \Phi_L(\mathbf{k}) \Phi_L^*(\mathbf{k}') \rangle = (2\pi)^3 \delta_D(\mathbf{k} - \mathbf{k}') P_{\Phi\Phi}(k)$.

A. 21-cm Trispectrum

Using the multiple moments of the 21-cm background a_{lm} , we can construct the angular average trispectrum, which is a rotationally invariant correlation function [40]. We define this the usual way such that

$$\langle a_{l_1 m_1} a_{l_2 m_2} a_{l_3 m_3} a_{l_4 m_4} \rangle = \sum_{LM} (-1)^M \begin{pmatrix} l_1 & l_2 & L \\ m_1 & m_2 & -M \end{pmatrix} \begin{pmatrix} l_3 & l_4 & L \\ m_3 & m_4 & M \end{pmatrix} T_{l_3 l_4}^{l_1 l_2}(L), \quad (9)$$

where $T_{l_3 l_4}^{l_1 l_2}(L)$ is the angular averaged trispectrum. Here l_1, l_2, l_3, l_4 form a quadrilateral with L as the length of the diagonal and matrices are the Wigner 3- j symbols. These symbols are non-zero under these conditions: $|l_1 - l_2| \leq L \leq l_1 + l_2$, $|l_3 - l_4| \leq L \leq l_3 + l_4$, $l_1 + l_2 + L = \text{even}$, $l_3 + l_4 + L = \text{even}$, $m_1 + m_2 = M$, and $m_3 + m_4 = -M$.

The angular averaged trispectrum has two parts involving a connected piece associated with non-Gaussianity and an disconnected part that is non-zero even if fluctuations are Gaussian with $T_{\text{tot}l_3l_4}^{l_1l_2}(L) = T_{G_{l_3l_4}}^{l_1l_2}(L) + T_{\text{NG}_{l_3l_4}}^{l_1l_2}(L)$ [40]. The Gaussian disconnected part is

$$T_{G_{l_3l_4}}^{l_1l_2}(L) = (-1)^{l_1+l_3} \sqrt{(2l_1+1)(2l_3+1)} C_{l_1} C_{l_3} \delta_{l_1l_2} \delta_{l_3l_4} \delta_{L0} \\ + (2L+1) C_{l_1} C_{l_2} [(-1)^{l_1+l_2+L} \delta_{l_1l_3} \delta_{l_2l_4} + \delta_{l_1l_4} \delta_{l_2l_3}]. \quad (10)$$

The connected part can be simplified based on permutation symmetries as

$$T_{\text{NG}_{l_3l_4}}^{l_1l_2}(L) = P_{l_3l_4}^{l_1l_2}(L) + (2L+1) \sum_{L'} \left[(-1)^{l_2+l_3} \begin{Bmatrix} l_1 & l_2 & L \\ l_4 & l_3 & L' \end{Bmatrix} P_{l_2l_4}^{l_1l_3}(L') + (-1)^{L+L'} \begin{Bmatrix} l_1 & l_2 & L \\ l_3 & l_4 & L' \end{Bmatrix} P_{l_3l_2}^{l_1l_4}(L') \right], \quad (11)$$

where

$$P_{l_3l_4}^{l_1l_2}(L) = \mathcal{T}_{\text{NG}_{l_3l_4}}^{l_1l_2}(L) + (-1)^{l_1+l_2+l_3+l_4+2L} \mathcal{T}_{\text{NG}_{l_4l_3}}^{l_2l_1}(L) + (-1)^{l_3+l_4+L} \mathcal{T}_{\text{NG}_{l_4l_3}}^{l_1l_2}(L) + (-1)^{l_1+l_2+L} \mathcal{T}_{l_3l_4}^{l_2l_1}(L). \quad (12)$$

In above, matrices are now the Wigner $6j$ symbol and $\mathcal{T}_{l_3l_4}^{l_1l_2}(L)$ is what is described as the reduced trispectrum in the literature [32, 40, 41].

To generate a non-Gaussianity in the 21-cm background that will lead to a trispectrum, we assume quadratic and cubic corrections to the Newtonian curvature such that

$$\Phi(\mathbf{x}) = \Phi_L(\mathbf{x}) + f_{\text{NL}} [\Phi_L^2(\mathbf{x}) - \langle \Phi_L^2(\mathbf{x}) \rangle] + f_2 \Phi_L^3(\mathbf{x}) \quad (13)$$

when $\Phi_L(\mathbf{x})$ is the linear and Gaussian perturbation and f_{NL} and f_2 are the coupling parameters, which may or may not be scale dependent. Note that f_2 is also identified in some publications as g_{NL} [30] though we follow the notation of Ref. [32]. Under this description, existing WMAP data limits $-30 < f_{\text{NL}} < 74$ at the 1σ confidence [35], while with an ideal CMB experiment fundamentally limited by cosmic variance one can constrain $|f_{\text{NL}}| < 3$ [19]. The angular bispectrum of 21-cm fluctuations, especially if measured between $z \sim 30$ and $z \sim 75$ prior to the formation of first sources and out to angular scales corresponding to multipoles of $\sim 10^4$ can be used to limit $|f_{\text{NL}}| < 0.1$ [17]. This is well below the standard expectations for f_{NL} even after accounting for second-order evolution during horizon exit and re-entry [26]. There are no useful observational limits on f_2 and no estimate on how well f_2 can be established with the CMB trispectrum.

In Fourier space, we can decompose equation (13) as

$$\Phi(\mathbf{k}) = \Phi_L(\mathbf{k}) + f_{\text{NL}} \Phi_2(\mathbf{k}) + f_2 \Phi_3(\mathbf{k}), \quad (14)$$

with

$$\Phi_2(\mathbf{k}) = \int \frac{d^3 \mathbf{k}_1}{(2\pi)^3} \Phi_L(\mathbf{k} + \mathbf{k}_1) \Phi_L^*(\mathbf{k}_1) - (2\pi)^3 \delta(\mathbf{k}) \int \frac{d^3 \mathbf{k}_1}{(2\pi)^3} P_{\Phi\Phi}(\mathbf{k}_1) \quad (15)$$

$$\Phi_3(\mathbf{k}) = \int \frac{d^3 \mathbf{k}_1}{(2\pi)^3} \int \frac{d^3 \mathbf{k}_2}{(2\pi)^3} \Phi_L^*(\mathbf{k}_1) \Phi_L^*(\mathbf{k}_2) \Phi_L(\mathbf{k}_1 + \mathbf{k}_2 + \mathbf{k}). \quad (16)$$

Using these, the reduced connected trispectrum can be written as

$$\langle \Phi(\mathbf{k}_1) \Phi(\mathbf{k}_2) \Phi(\mathbf{k}_3) \Phi(\mathbf{k}_4) \rangle_c = (2\pi)^3 \int d^3 K \delta_D(\mathbf{k}_1 + \mathbf{k}_2 + \mathbf{K}) \delta_D(\mathbf{k}_3 + \mathbf{k}_4 - \mathbf{K}) \mathcal{T}_{\Phi}(\mathbf{k}_1, \mathbf{k}_2, \mathbf{k}_3, \mathbf{k}_4; \mathbf{K}) \quad (17)$$

with two terms involving

$$\mathcal{T}_{\Phi}^{(2)}(\mathbf{k}_1, \mathbf{k}_2, \mathbf{k}_3, \mathbf{k}_4; \mathbf{K}) = 4f_{\text{NL}}^2 P_{\Phi\Phi}(K) P_{\Phi\Phi}(k_1) P_{\Phi\Phi}(k_3) \\ \mathcal{T}_{\Phi}^{(3)}(\mathbf{k}_1, \mathbf{k}_2, \mathbf{k}_3, \mathbf{k}_4; \mathbf{K}) = f_2 [P_{\Phi\Phi}(k_2) P_{\Phi\Phi}(k_3) P_{\Phi\Phi}(k_4) + P_{\Phi\Phi}(k_2) P_{\Phi\Phi}(k_1) P_{\Phi\Phi}(k_4)]. \quad (18)$$

Using the 21-cm transfer function defined in equation (7) and using equation (17), we write

$$\langle a_{l_1 m_1} a_{l_2 m_2} a_{l_3 m_3} a_{l_4 m_4} \rangle = (4\pi)^4 (-i)^{\sum l_i} \int \frac{d^3 \mathbf{k}_1}{(2\pi)^3} \dots \int \frac{d^3 \mathbf{k}_4}{(2\pi)^3} \int d^3 K \\ \times (2\pi)^3 \delta_D(\mathbf{k}_1 + \mathbf{k}_2 + \mathbf{K}) \delta_D(\mathbf{k}_3 + \mathbf{k}_4 - \mathbf{K}) \mathcal{T}_{\Phi}(\mathbf{k}_1, \mathbf{k}_2, \mathbf{k}_3, \mathbf{k}_4; \mathbf{K}) g_{21\text{cm}, l_1}(k_1) g_{21\text{cm}, l_2}(k_2) g_{21\text{cm}, l_3}(k_3) g_{21\text{cm}, l_4}(k_4) \\ \times Y_{l_1 m_1}^*(\hat{\mathbf{k}}_1) Y_{l_2 m_2}^*(\hat{\mathbf{k}}_2) Y_{l_3 m_3}^*(\hat{\mathbf{k}}_3) Y_{l_4 m_4}^*(\hat{\mathbf{k}}_4). \quad (19)$$

We simplify further by expanding the δ_D functions, for example,

$$\delta_D(\mathbf{k}_3 + \mathbf{k}_4 - \mathbf{K}) = \int \frac{d^3 \mathbf{r}}{(2\pi)^3} e^{-i\mathbf{r} \cdot (\mathbf{k}_3 + \mathbf{k}_4 - \mathbf{K})}, \quad (20)$$

and combining with the Rayleigh expansion of a plane wave

$$e^{i\mathbf{r} \cdot \mathbf{k}} = (4\pi) \sum_{lm} i^l j_l(kr) Y_{lm}^*(\hat{\mathbf{k}}) Y_{lm}^*(\hat{\mathbf{r}}) \quad (21)$$

to simplify the reduced trispectrum of 21-cm anisotropies as

$$\begin{aligned} \mathcal{T}_{\text{NG}l_3l_4}^{l_1l_2}(L) &= \left(\frac{2}{\pi}\right)^5 \int k_1^2 dk_1 \dots \int k_4^2 dk_4 \int K^2 dK \int r_1^2 dr_1 \int r_2^2 dr_2 \mathcal{T}_\Phi(\mathbf{k}_1, \mathbf{k}_2, \mathbf{k}_3, \mathbf{k}_4; \mathbf{K}) \\ &\times g_{21\text{cm},l_1}(k_1) g_{21\text{cm},l_2}(k_2) g_{21\text{cm},l_3}(k_3) g_{21\text{cm},l_4}(k_4) j_{l_1}(k_1 r_1) j_{l_2}(k_2 r_1) j_{l_3}(k_3 r_2) j_{l_4}(k_4 r_2) j_L(K r_1) j_L(K r_2) h_{l_1 L L_2} h_{l_3 L L_4}, \end{aligned} \quad (22)$$

where

$$h_{l_1 L_2 L} = \sqrt{\frac{(2l_1 + 1)(2l_2 + 1)(2L + 1)}{4\pi}} \begin{pmatrix} l_1 & l_2 & L \\ 0 & 0 & 0 \end{pmatrix}. \quad (23)$$

Substituting for the reduced trispectrum of Newtonian curvature, and similar to the CMB trispectrum [32, 41], the reduced trispectrum of 21-cm anisotropies can be written with two contributions from second- and third-order corrections as

$$\begin{aligned} \mathcal{T}_{\text{NG}l_3l_4}^{l_1l_2}(L) &= 4f_{\text{NL}}^2 \int r_1^2 dr_1 \int r_2^2 dr_2 F_L(r_1, r_2) \alpha_{l_1}(r_1) \beta_{l_2}(r_1) \alpha_{l_3}(r_2) \beta_{l_4}(r_2) h_{l_1 l_2 L} h_{l_3 l_4 L} \\ &+ f_2 \int r^2 dr \beta_{l_2}(r) \beta_{l_4}(r) [\mu_{l_1}(r) \beta_{l_3}(r) + \beta_{l_1}(r) \mu_{l_3}(r)] h_{l_1 l_2 L} h_{l_3 l_4 L} \end{aligned} \quad (24)$$

where

$$\begin{aligned} F_L(r_1, r_2) &= \frac{2}{\pi} \int k^2 dk P_{\Phi\Phi}(k) j_L(kr_1) j_L(kr_2) \\ \alpha_l(r) &= \frac{2}{\pi} \int k^2 dk g_{21\text{cm},l}(k) j_l(kr) \\ \beta_l(r) &= \frac{2}{\pi} \int k^2 dk P_{\Phi\Phi}(k) g_{21\text{cm},l}(k) j_l(kr) \\ \mu_l(r) &= \frac{2}{\pi} \int k^2 dk g_{21\text{cm},l}(k) j_l(kr). \end{aligned} \quad (25)$$

B. 3-1 power spectrum

Instead of measuring the full trispectrum to extract information on the non-Gaussianity of primordial perturbations captured by f_{NL} and f_2 , we consider a compact statistic that measures non-Gaussian information but can be described as a higher order 2-point statistic. For this purpose, we introduce the three-to-one correlator analogous to the two-to-one correlator of Ref. [34] and applied to limit f_{NL} from WMAP in Ref. [35]. This statistic is

$$\begin{aligned} W(\hat{\mathbf{n}}, \hat{\mathbf{m}}) &\equiv \langle \hat{T}_b^3(\hat{\mathbf{n}}) T_b(\hat{\mathbf{m}}) \rangle \\ &= \sum_{l_1 m_1 l_2 m_2} \langle a_{l_1 m_1}^3 a_{l_2 m_2}^* \rangle Y_{l_1}^{m_1}(\hat{\mathbf{n}}) Y_{l_2}^{m_2*}(\hat{\mathbf{m}}), \end{aligned} \quad (26)$$

where $a_{lm}^3 = \int d\hat{\mathbf{n}} \hat{T}_b^3(\hat{\mathbf{n}}) Y_l^{m*}(\hat{\mathbf{n}})$, where $\hat{T}_b(\hat{\mathbf{n}})$ is the 21-cm brightness temperature with the filter described below applied in multipole space. We note that this statistic has been recently discussed in the context of separating lensing and kinetic Sunyaev-Zel'dovich contributions to arcminute scale CMB anisotropies [42].

Similar to the filtered two-to-one angular power spectrum [17, 34], the three-to-one cubic angular power spectrum is

$$\langle a_{lm}^3 a_{l'm'}^* \rangle = X_l^{\text{tot}} \delta_{ll'} \delta_{mm'}, \quad (27)$$

where

$$X_l^{\text{tot}} = \frac{1}{\sqrt{2l+1}} \sum_{l_1 l_2 l_3 L} \frac{(-1)^{l_1+l_2+L}}{(2L+1)} T_{\text{tot} l_3 l}^{l_1 l_2}(L) w_{l_1 l_2 l_3 | l, L} h_{l_1 l_2 L} h_{l_3 l L}, \quad (28)$$

where $w_{l_1 l_2 l_3 | l, L}$ is the form of the filter function that applies to the cubic field to optimize the detection of any particular form of the underlying trispectrum. In real space, this filter can be simply described as $a_{lm}^3 = \int d\hat{\mathbf{n}} \hat{T}_b^3(\hat{\mathbf{n}}) W_1(\hat{\mathbf{n}}) W_2(\hat{\mathbf{n}}) W_3(\hat{\mathbf{n}}) Y_l^{m*}(\hat{\mathbf{n}})$ where W_1 to W_3 are real space filters that are applied to the three maps of the same field that are multiplied together. In above X_l note that contributions come from both the unconnected Gaussian part of the trispectrum T_g and the connected non-Gaussian part of the trispectrum T_c . For simplicity, we identify separately X_l^{prim} and X_l^{grav} as the contributions resulting from the trispectra of the density field generated by primordial density perturbations (equation 24) and the subsequent non-linear gravitational evolution of the density field (see below), respectively. Here, we are primarily interested in detecting the non-Gaussian information contained in the non-Gaussian part of the trispectrum produced by primordial non-Gaussianities or X_l^{prim} . With the Gaussian contribution to the trispectrum, the total three-to-one angular power spectrum can be written as $X_l^{\text{tot}} = X_l^{\text{prim}} + X_l^{\text{grav}} + X_l^{\text{Gaussian}}$.

Substituting Eq. 10 in in Eq. 19 we derive a simplified expression for X_l^{Gaussian} as

$$X_l^{\text{Gaussian}} = \frac{\sqrt{2l+1}}{4\pi} C_l \sum_{l_1 L} (2l_1+1) C_{l_1} \left[w_{l l_1 l | l, L} \delta_{L0} + (2L+1) \begin{pmatrix} l_1 & l & L \\ 0 & 0 & 0 \end{pmatrix}^2 \{ w_{l l_1 l | l, L} + w_{l l_1 l_1 | l, L} \} \right]. \quad (29)$$

If the filter function $w_{l_1 l_2 l_3 | l, L}$ is designed such that it is equal to zero if any of (l_1, l_2, l_3) is equal to another then $X_l^{\text{Gaussian}} = 0$ and there is no contribution to the three-to-one angular power spectrum from the Gaussian term.

The variance of the three-to-one power spectrum calculated from $\langle X_l X_l' \rangle - \langle X_l \rangle^2$ with

$$\langle X_l X_l' \rangle = \frac{1}{(2l+1)(2l'+1)} \sum_{mm'} \langle a_{lm}^3 a_{lm}^{*3} a_{l'm}^{3*} a_{l'm} \rangle, \quad (30)$$

is

$$(2l+1)N_l^2 = \left(X_l^{\text{prim}} \right)^2 + \left(X_l^{\text{grav}} \right)^2 + \left(X_l^{\text{Gaussian}} \right)^2 + \frac{C_l^{\text{tot}}}{(2l+1)} \sum_{l_1 l_2 l_3 L} \frac{w_{l_1 l_2 l_3 | l, L}^2}{(2L+1)} C_{l_1}^{\text{tot}} C_{l_2}^{\text{tot}} C_{l_3}^{\text{tot}} h_{l_1 l_2 L}^2 h_{l_3 l L}^2, \quad (31)$$

and we have ignored the covariance generated by non-Gaussian terms involving three- to eight-point correlations of a_{lm} .

To optimize the detection of X_l^{prim} , under the assumption that $X_l^{\text{grav}} < X_l^{\text{prim}}$ first, we find the shape of the filter that maximizes the signal-to-noise ratio for its detection is

$$w_{l_1 l_2 l_3 | l, L} = \frac{(-1)^{l_1+l_2+L}}{h_{l_1 l_2 L} h_{l_3 l L}} \frac{T_c^{\text{prim} l_1 l_2}}{C_{l_1} C_{l_2} C_{l_3}}, \quad (32)$$

with the additional constraint that $w_{l_1 l_2 l_3 | l, L} = 0$ if two of (l_1, l_2, l_3, l) are equal.

With the filter applied, the noise related to X_l^{prim} is

$$N_l^{\text{tot}} = \left[\frac{(X_l^{\text{grav}})^2}{2l+1} + \frac{C_l^{\text{tot}}}{(2l+1)^2} \sum_{l_1 l_2 l_3 L} \frac{w_{l_1 l_2 l_3 | l, L}^2}{(2L+1)} C_{l_1}^{\text{tot}} C_{l_2}^{\text{tot}} C_{l_3}^{\text{tot}} h_{l_1 l_2 L}^2 h_{l_3 l L}^2 \right]^{1/2}. \quad (33)$$

With the assumption that $X_l^{\text{grav}} \approx 0$ then maximum signal-to-noise ratio for a detection of X_l^{prim} with a noise spectrum of N_l^{tot} is

$$\left(\frac{S}{N} \right)^2 = \sum_{l_1 > l_2 > l_3 > l, L} \frac{|T_c^{\text{prim} l_1 l_2}(L)|^2}{(2L+1) C_{l_1}^{\text{tot}} C_{l_2}^{\text{tot}} C_{l_3}^{\text{tot}} C_l^{\text{tot}}}. \quad (34)$$

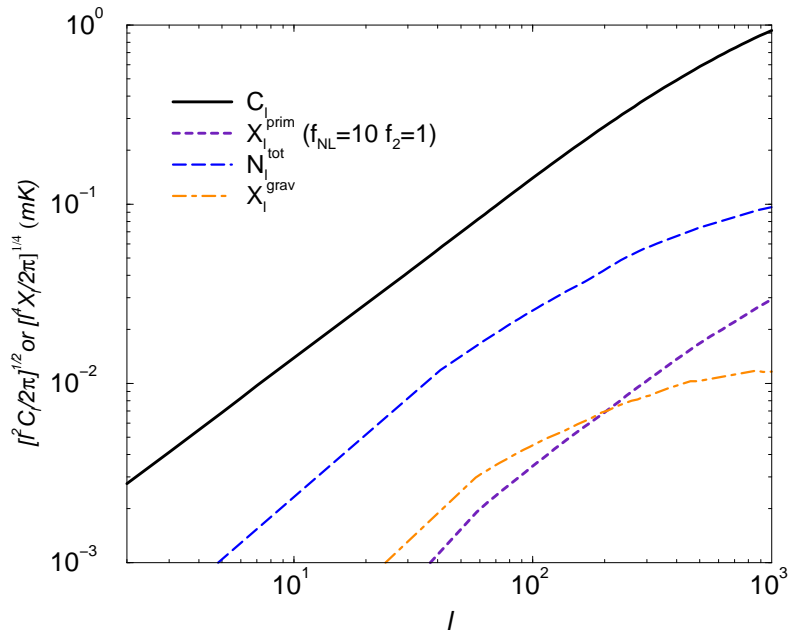


FIG. 1: The power spectrum of 21-cm anisotropies (top solid line) and the angular power spectrum of the projected three-to-one correlator described in the paper as a probe of the 21 cm trispectrum. In addition to X_l^{prim} with $f_{\text{NL}} = 10$ and $f_2 = 1$, we also show X_l^{grav} and N_l .

This is the same signal-to-noise ratio for a detection of the trispectrum generated by primordial non-Gaussianity. However, X_l^{grav} is not necessarily zero and with the same filter applied in the presence of non-negligible non-Gaussianity from non-linear density perturbations, there is a residual contribution to X_l that reduces the overall signal-to-noise ratio to be below that of the maximal value for a detection of the primordial trispectrum alone. In this sense, in the presence of secondary non-Gaussian signal, the filter in equation (32) is non-optimal and could potentially be redesigned to improve the overall signal-to-noise ratio for a detection of X_l^{prim} . While we do not make such an attempt here, in estimating the signal-to-noise ratio, we do account for the contamination from X_l^{grav} and the overall signal-to-noise ratios we calculated from X_l^{prim} and N_l is below the signal-to-noise ratio given in equation (34).

This degradation in the signal-to-noise ratio comes from the cross-correlation of trispectra of primordial non-Gaussianity (as used in the filter) and the non-Gaussianity generated by gravitational evolution of density perturbations. To understand this confusion associated with non-linear gravitational evolution, we also calculate X_l^{grav} following the derivation of $T_c^{\text{grav}l_1l_2}_{l_3l_4}(L)$ as described in the Appendix. Since $w_{l_1l_2l_3|l,L}$ is defined in terms of the primordial trispectrum, $X_l^{\text{grav}} \propto \sum_{l_1l_2l_3L} T_c^{\text{prim}l_1l_2}_{l_3l}(L) \times T_c^{\text{grav}l_1l_2}_{l_3l}(L)$ while $X_l^{\text{prim}} \propto \sum_{l_1l_2l_3L} |T_c^{\text{prim}l_1l_2}_{l_3l}(L)|^2$. Since modes of $T_c^{\text{grav}l_1l_2}_{l_3l}(L)$ do not align with those of $T_c^{\text{prim}l_1l_2}_{l_3l}(L)$ the former sum has cancellations and in general we do expect X_l^{grav} to be at the same order as X_l^{prim} or below.

The dominant contribution to N_l^{tot} is not X_l^{grav} but is the Gaussian variance captured by the second term of equation (33). This statement is independent of f_{NL} and f_2 . If stated differently, when properly filtered to search for the primordial non-Gaussianity, the main confusion for detecting primordial signal is not the non-Gaussianity generated by non-linear perturbations but rather the Gaussian covariance associated with the statistical measurement of X_l^{prim} . In practice, the measurement of X_l^{prim} is likely to be further confused by the non-Gaussianity of foregrounds, which we have mostly ignored in the present discussion. Unfortunately, little is known about the expected level of the foreground intensity in the low radio frequency range of interest. Techniques have been suggested and discussed to remove foregrounds below the detector noise levels [38, 39] and the filtering process we have outlined will further reduce the confusion from the remaining residual foregrounds. This is clearly a topic for further study once data become available with first-generation interferometers [47].

III. RESULTS AND DISCUSSION

In Fig. 1 we summarize the power-spectrum of 21-cm anisotropies generated by the neutral hydrogen distribution at a redshift of 100 with a bandwidth for observations of 1 MHz. Here, we also plot X_l^{prim} , X_l^{grav} , and N_l^{tot} for the same redshift with the optimal filter applied with $f_{\text{NL}} = 10$ and $f_2 = 1$ as the non-Gaussian scale-independent amplitude of the primordial second- and third-order curvature perturbations, respectively. As shown, $N_l^{\text{tot}} > X_l^{\text{grav}}$, suggesting that the noise term is dominated by the Gaussian variance (second term in equation 33). This statement is independent of f_{NL} and f_2 and thus the non-Gaussian detection is dominated by the Gaussian term in N_l regardless of what is assumed about non-Gaussianity. Note that we have estimated N_l^{tot} in Fig. 1 under the assumption that observations are limited only by the cosmic variance and not accounting for any instrumental noise variance, which will also lead to a cut-off in l out to which we can make measurements. Using the cosmic variance alone allows us to establish the potentially achievable limit and compare directly with cosmic variance limit with CMB data. When calculating X_l^{prim} and X_l^{grav} in equation (28) we set maximum value of L in the sum associated with $T^{l_1 l_2 l_3}(L)$ to be $L_{\text{max}} = 100$. We tested our calculation for $L_{\text{max}} = 150$ and found results to be within a percent, but such a higher value slows the numerical calculation significantly. Finally, due to computational limitations of the numerical calculation, we restrict estimate of X_l to $l = 10^3$.

In Fig. 1 when calculating X_l^{grav} , following the derivation in the Appendix and the discussion there, we use the exact analytical result for the 2-2 trispectrum of the density field with the mode coupling captured by $F_2(\mathbf{k}_1, \mathbf{k}_2)$ [43, 44]. For the 3-1 trispectrum of the density field under non-linear gravitational evolution, given that an analytical result for the angular trispectrum is cumbersome, we use the angular averaged value for $F_3(\mathbf{k}_1, \mathbf{k}_2, \mathbf{k}_3)$. We refer the reader to the Appendix for details.

In Fig. 2 we summarize the estimate related to signal-to-noise ratio for a detection of X_l^{prim} as a function of l . The typical signal-to-noise ratio, when measurements are out to a multipole of 10^3 , is at the level of ~ 0.5 if one assumes that the coupling parameters $f_{\text{NL}} = 10$ and $f_2 = 3$ for 21-cm observations centered at a redshift of 100 over a bandwidth of 1 MHz. The signal-to-noise ratio for the case with $f_{\text{NL}} = 0$ and $f_2 = 3$ is ~ 0.03 . Since $S/N \propto f_2$ when $f_{\text{NL}} = 0$, out to $l = 10^3$, a signal-to-noise ratio of 1 is achieved if $f_2 \sim 10^2$. While there are neither strong theoretical motivations on the expected value of f_2 nor a real bound on its value from existing data, it is likely that with 21-cm data one can constrain f_2 down to a level well below this value for a single redshift. This is due to the fact that 21-cm observations lead to measurements at multiple redshifts, though one cannot make arbitrarily small bandwidths to improve the detection since at scales below a few Mpc, anisotropies in one redshift bin will be correlated with those in adjacent bins [39]. For example, if 21-cm observations are separated to 30 independent bins over the redshift interval 50 to 100 (as can be achieved with 1 MHz bandwidths), then an approximate estimate of the cumulative signal-to-noise ratio, $S/N = \sqrt{\sum_z [S/N(z)]^2}$, is $\sim 0.15(f_2/3)$ if $f_{\text{NL}} = 0$. In return, one can potentially probe f_{NL} values as low as 20 roughly out to $l_{\text{max}} \sim 10^3$. With the first-generation radio interferometers, we would at most survey 1% of the sky. Assuming instrument noise is dominating at multipoles above 10^3 between 30 MHz and 60 MHz at 1 MHz bandwidths (corresponding to redshifts 30 to 100), we find a signal-to-noise ratio of $5 \times 10^{-3} f_2$, which could lead to a limit on f_2 of order 200.

Above discussion on the application of X_l^{prim} assumes that $f_{\text{NL}} = 0$. Since $X_l^{\text{prim}} \propto f_{\text{NL}}^2$, if f_{NL} is greater than one, the overall signal-to-noise ratio for the detection of the three-to-one angular power spectrum is increased and the dominant contribution to X_l^{prim} comes from the coupling associated with f_{NL} and not f_2 . In the case when $f_2 = 0$, the f_{NL} one probes with the trispectrum can be related to τ_{NL} of Refs. [31, 33] for the primordial trispectrum. In Fig. 2, we show the signal-to-noise ratio with $f_{\text{NL}} = 10$ and $f_2 = 3$. Since in this case f_{NL} term dominates, this provides an approximate estimate of the signal-to-noise ratio for f_{NL} with the trispectrum. Using a single redshift bin out to $l_{\text{max}} \sim 10^3$, 21-cm observations achieve a signal-to-noise ratio of 1 if $f_{\text{NL}} \sim 15$. This in return constraints $\tau_{\text{NL}} \lesssim 300$. Assuming 30 redshift bins over the redshift interval 50 to 100, assuming $f_2 = 0$, we find that one can constrain $\tau_{\text{NL}} < 50$. This result is only out to $l_{\text{max}} = 10^3$, but since 21-cm observations are not damped as in the case of CMB observations, higher resolution data can improve limits on both f_2 and τ_{NL} significantly especially if observations can be pushed to $l > 10^4$.

While a detection of the CMB angular trispectrum has been motivated as a way to constrain f_{NL} or τ_{NL} [32], this is probably not necessary with 21-cm data. Once radio interferometers start probing the redshift interval of 50 to 100, the angular bispectrum, which can be probed with the two-to-one angular power spectrum [17], can limit $f_{\text{NL}} < 0.1$. This will facilitate a separation of the contribution to the three-to-one power spectrum from f_{NL} and f_2 . While we have assumed that f_{NL} and f_2 are momentum independent, it is likely that for specific models of inflation, these coupling terms are momentum dependent [46] and then the ability to separate f_{NL} and f_2 by combining 21-cm bispectrum and trispectrum information with the two-to-one and three-to-one correlator respectively will strongly depend on the exact momentum dependence of the coupling factors. We leave such a study for future research. While measuring f_2 is well motivated, one can also test the consistency between f_{NL} probed by the bispectrum and the τ_{NL} from the trispectrum related to the slow-roll inflation predictions for the non-Gaussianity. While we have not

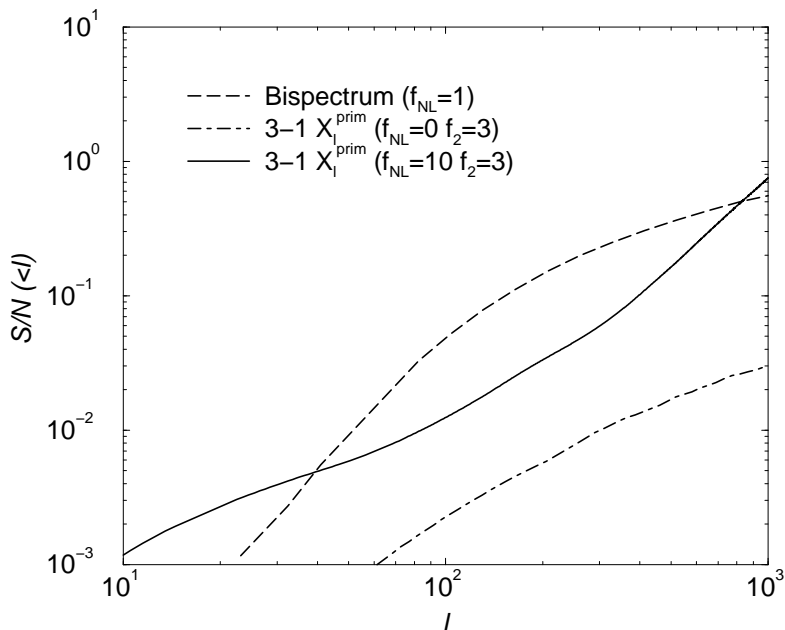


FIG. 2: Signal-to-noise ratio for a detection of X_l^{prim} with $f_{\text{NL}} = 10$ and $f_2 = 3$ (solid line) and $f_{\text{NL}} = 0$ and $f_2 = 3$ (dot-dashed line). For reference, we show the signal-to-noise ratio associated with the detection of the full 21-cm bispectrum with a dashed line.

discussed the extent to which this consistency relation can be established with upcoming experiments after taking into account of instrumental noise it will also be useful to return to such a calculation in the future once 21-cm observations begin to probe the universe at $z > 10$.

IV. SUMMARY

The 21-cm anisotropies from the neutral hydrogen distribution prior to the era of reionization is expected to be more sensitive to primordial non-Gaussianity than the cosmic microwave background due to both the three-dimensional nature of the 21-cm signal and the lack of a damping tail at arcminute angular scales. Previous calculations have discussed the extent to which 21-cm bispectrum can be used as a probe of primordial non-Gaussianity at the two-point level with an non-Gaussianity parameter f_{NL} [17, 18].

Here, we extend these calculations to discuss the possibility to use a four point statistic of the 21-cm background as a probe of the primordial non-Gaussianity associated with the trispectrum. We have calculated the angular trispectrum of the 21-cm background anisotropies and have introduced the three-to-one correlator and the corresponding angular power spectrum as a probe of the primordial trispectrum captured by both f_{NL} and the third order non-Gaussianity parameter f_2 (described in some publications as g_{NL}). Since the primordial non-Gaussianity is confused with a non-Gaussian signal in the 21-cm background generated by the non-linear evolution of the density perturbations under gravitational evolution, we have discussed way to separate the two using an optimal filter. While with the angular bispectrum of 21-cm anisotropies one can limit the second order corrections to the primordial fluctuations as low as $f_{\text{NL}} \sim 0.1$ below the value of ~ 1 expected for inflationary models, using the trispectrum information we suggest that one can constrain third order coupling term f_2 to about few tens. If f_{NL} is large, it could potentially be possible to test the consistency between f_{NL} from the bispectrum and the slow-roll non-Gaussianity τ_{NL} at the four-point level with the relation $\tau_{\text{NL}} = (6f_{\text{NL}}/5)^2$. We hope to return to such a detailed study in the future.

Acknowledgments

This work was supported in part by NSF CAREER AST-0645427 at UC Irvine and by the Moore Foundation at Caltech. We thank David Lyth for motivating us to calculate the 21 cm trispectrum.

V. APPENDIX

Here we discuss the trispectrum from the non-linear density field. The trispectrum is generated by both second and third-order perturbative corrections to the density fluctuations:

$$\delta(\mathbf{k}) = \delta^{(1)}(\mathbf{k}) + \delta^{(2)}(\mathbf{k}) + \delta^{(3)}(\mathbf{k}), \quad (35)$$

where $\delta^{(1)}(\mathbf{k}) = \delta_{\text{lin}}(\mathbf{k})$ is the linear density perturbation and

$$\delta^{(2)}(\mathbf{k}) = \int \frac{d^3\mathbf{k}_1}{(2\pi)^3} \int \frac{d^3\mathbf{k}_2}{(2\pi)^3} (2\pi)^3 \delta_D(\mathbf{k}_1 + \mathbf{k}_2 - \mathbf{k}) \delta_{\text{lin}}(\mathbf{k}_1) \delta_{\text{lin}}(\mathbf{k}_2) F_2(\mathbf{k}_1, \mathbf{k}_2) \quad (36)$$

$$\delta^{(3)}(\mathbf{k}) = \int \frac{d^3\mathbf{k}_1}{(2\pi)^3} \int \frac{d^3\mathbf{k}_2}{(2\pi)^3} (2\pi)^3 \int \frac{d^3\mathbf{k}_3}{(2\pi)^3} (2\pi)^3 \delta_D(\mathbf{k}_1 + \mathbf{k}_2 + \mathbf{k}_3 - \mathbf{k}) \delta_{\text{lin}}(\mathbf{k}_1) \delta_{\text{lin}}(\mathbf{k}_2) \delta_{\text{lin}}(\mathbf{k}_3) F_3(\mathbf{k}_1, \mathbf{k}_2, \mathbf{k}_3),$$

where $F_2(\mathbf{k}_1, \mathbf{k}_2)$ and $F_3(\mathbf{k}_1, \mathbf{k}_2, \mathbf{k}_3)$ are derived in Ref. [43, 44].

The reduced trispectrum of density perturbations $\langle \delta(\mathbf{k}_1) \delta(\mathbf{k}_2) \delta(\mathbf{k}_3) \delta(\mathbf{k}_4) \rangle$ can be written in terms of the connected piece as

$$\langle \delta(\mathbf{k}_1) \delta(\mathbf{k}_2) \delta(\mathbf{k}_3) \delta(\mathbf{k}_4) \rangle = (2\pi)^3 \int d^3K \delta_D(\mathbf{k}_1 + \mathbf{k}_2 + \mathbf{K}) \delta_D(\mathbf{k}_3 + \mathbf{k}_4 - \mathbf{K}) \mathcal{T}_\delta(\mathbf{k}_1, \mathbf{k}_2, \mathbf{k}_3, \mathbf{k}_4; \mathbf{K}) \quad (37)$$

with two terms involving

$$\begin{aligned} \mathcal{T}_\delta^{(2)}(\mathbf{k}_1, \mathbf{k}_2, \mathbf{k}_3, \mathbf{k}_4; \mathbf{K}) &= 4F_2(\mathbf{k}_1, \mathbf{K}) F_2(\mathbf{k}_3, \mathbf{K}) P_\delta(K) P_\delta(k_1) P_\delta(k_3) \\ \mathcal{T}_\delta^{(3)}(\mathbf{k}_1, \mathbf{k}_2, \mathbf{k}_3, \mathbf{k}_4; \mathbf{K}) &= F_3(\mathbf{k}_2, \mathbf{k}_3, \mathbf{k}_4) P_\delta(k_2) P_\delta(k_3) P_\delta(k_4) + F_3(\mathbf{k}_2, \mathbf{k}_1, \mathbf{k}_4) P_\delta(k_2) P_\delta(k_1) P_\delta(k_4), \end{aligned} \quad (38)$$

where

$$F_2(\mathbf{k}_1, \mathbf{k}_2) = \frac{5}{7} + \frac{\mathbf{k}_1 \cdot \mathbf{k}_2}{2k_2^2} + \frac{\mathbf{k}_1 \cdot \mathbf{k}_2}{2k_1^2} + \frac{2}{7} \left(\frac{\mathbf{k}_1 \cdot \mathbf{k}_2}{k_1 k_2} \right)^2, \quad (39)$$

and $F_3(\mathbf{k}_1, \mathbf{k}_2, \mathbf{k}_3)$ is derived in the Appendix of Ref. [43].

To calculate the angular trispectrum of 21-cm anisotropies we make use of the 21-cm transfer function defined in equation (7) and equation (37) to write

$$\begin{aligned} \langle a_{l_1 m_1} a_{l_2 m_2} a_{l_3 m_3} a_{l_4 m_4} \rangle &= (4\pi)^4 (-i)^{\sum l_i} \int \frac{d^3\mathbf{k}_1}{(2\pi)^3} \dots \int \frac{d^3\mathbf{k}_4}{(2\pi)^3} \int d^3K \\ &\times (2\pi)^3 \delta_D(\mathbf{k}_1 + \mathbf{k}_2 + \mathbf{K}) \delta_D(\mathbf{k}_3 + \mathbf{k}_4 - \mathbf{K}) \mathcal{T}_\phi(\mathbf{k}_1, \mathbf{k}_2, \mathbf{k}_3, \mathbf{k}_4; \mathbf{K}) g_{21\text{cm}, l_1}(k_1) g_{21\text{cm}, l_2}(k_2) g_{21\text{cm}, l_3}(k_3) g_{21\text{cm}, l_4}(k_4) \\ &\times Y_{l_1 m_1}^*(\hat{\mathbf{k}}_1) Y_{l_2 m_2}^*(\hat{\mathbf{k}}_2) Y_{l_3 m_3}^*(\hat{\mathbf{k}}_3) Y_{l_4 m_4}^*(\hat{\mathbf{k}}_4). \end{aligned} \quad (40)$$

The angular trispectrum associated with the $\delta^{(2)}$ term can be calculated numerically in a reasonable time, but the exact numerical calculation of the angular trispectrum of 21-cm anisotropies associated with $\delta^{(3)}$ term is slow. Here, we outline the analytical derivation of the trispectrum associated with the $\delta^{(2)}$ term, but for the $\delta^{(3)}$ term, following an approach similar to prior calculations of the non-Gaussianity associated with the trispectrum of gravitational evolution [45], we employ an approximation with the angular averaged value $R_b \equiv \langle F_3(\mathbf{k}_1, \mathbf{k}_2, \mathbf{k}_3) \rangle = 682/189$ [44] and ignore the exact mode coupling resulting from the F_3 term. This assumption allows us to write $\mathcal{T}_\delta^{(3)} = R_b [P(k_1)P(k_2)P(k_3) + \dots]$.

Compared to the derivation in Section II where the trispectrum from primordial perturbations involve a coupling term which is momentum-independent, the derivation of the trispectrum associated with non-linear evolution with a momentum-dependent term is tedious. We take multipole moments of the F_2 term

$$F_2(\mathbf{k}_1, \mathbf{k}_2) = (4\pi) \sum_{l_a m_a} F_{2, l_a}(k_1, k_2) Y_{l_a m_a}(\hat{\mathbf{k}}_1) Y_{l_a m_a}^*(\hat{\mathbf{k}}_2) \quad (41)$$

and since F_2 involves terms $(\mathbf{k}_1 \cdot \mathbf{k}_2)^n$ from $n = 0, 1, 2$, l_a takes the values of 0,1,2. We outline the contribution for a specific combination of (l_a, l_b) involving the expansion of the two F_2 terms, the trispectrum calculation generally involves a term of the form

$$\begin{aligned} \langle a_{l_1 m_1} a_{l_2 m_2} a_{l_3 m_3} a_{l_4 m_4} \rangle &= 4(4\pi)^6 (-i)^{\sum l_i} \int \frac{d^3\mathbf{k}_1}{(2\pi)^3} \dots \int \frac{d^3\mathbf{k}_1}{(2\pi)^3} \int d^3K \int \frac{d^3\mathbf{r}_1}{(2\pi)^3} \int \frac{d^3\mathbf{r}_2}{(2\pi)^3} \\ &\times \sum_{m_a m_b} Y_{l_a m_a}(\hat{\mathbf{k}}_1) Y_{l_a m_a}^*(\hat{\mathbf{K}}) Y_{l_b m_b}(\hat{\mathbf{k}}_3) Y_{l_b m_b}^*(\hat{\mathbf{K}}) F_{2, l_a}(k_1, K) F_{2, l_b}(k_3, K) P_\phi(K) P_\phi(k_1) P_\phi(k_3) \\ &\times e^{i\mathbf{r}_1 \cdot (\mathbf{k}_1 + \mathbf{k}_2 + \mathbf{K})} e^{i\mathbf{r}_2 \cdot (\mathbf{k}_3 + \mathbf{k}_4 - \mathbf{K})} g_{21\text{cm}, l_1}(k_1) g_{21\text{cm}, l_2}(k_2) g_{21\text{cm}, l_3}(k_3) g_{21\text{cm}, l_4}(k_4) Y_{l_1 m_1}^*(\hat{\mathbf{k}}_1) Y_{l_2 m_2}^*(\hat{\mathbf{k}}_2) Y_{l_3 m_3}^*(\hat{\mathbf{k}}_3) Y_{l_4 m_4}^*(\hat{\mathbf{k}}_4), \end{aligned} \quad (42)$$

which can be simplified with Rayleigh expansion of the plane waves followed by angular integrals to arrive after some tedious but straightforward algebra to

$$\begin{aligned}
& \langle a_{l_1 m_1} a_{l_2 m_2} a_{l_3 m_3} a_{l_4 m_4} \rangle = \tag{43} \\
& 4(4\pi)^{12} (-i)^{l_1+l_3} \int k_1^d k_1 \dots \int k_4^d dk_2 \int K^2 dK \int r_1^2 dr_1 \int r_2^2 dr_2 F_{2,l_a}(k_1, K) F_{2,l_b}(k_3, K) P_\phi(K) P_\phi(k_1) P_\phi(k_3) \\
& \times \sum_{m_a m_b L_1 M_1 L_2 M_2 L_3 M_3 L_4} i^{\sum L_i} (-1)^{m_1+m_2+m_3+M_1+L_4} g_{21\text{cm},l_1}(k_1) g_{21\text{cm},l_2}(k_2) g_{21\text{cm},l_3}(k_3) g_{21\text{cm},l_4}(k_4) \\
& \times j_{l_2}(k_2 r_1) j_{l_4}(k_4 r_2) j_{L_1}(k_1 r_1) j_{L_2}(k_3 r_2) j_{l_3}(K r_1) j_{L_4}(K r_2) h_{L_1 l_1 l_a} h_{L_2 l_3 l_b} h_{L_3 l_2 L_1} h_{L_4 l_4 L_2} \\
& \times \begin{pmatrix} L_1 & l_1 & l_a \\ M_1 & -m_1 & m_a \end{pmatrix} \begin{pmatrix} L_2 & l_3 & l_b \\ M_2 & -m_3 & m_b \end{pmatrix} \begin{pmatrix} L_3 & l_2 & L_1 \\ M_3 & -m_2 & -M_1 \end{pmatrix} \begin{pmatrix} L_4 & l_4 & L_2 \\ M_4 & m_4 & M_2 \end{pmatrix} \\
& \times \int d\hat{\mathbf{K}} Y_{l_a m_a}^*(\hat{\mathbf{K}}) Y_{l_b m_b}^*(\hat{\mathbf{K}}) Y_{L_3 M_3}^*(\hat{\mathbf{K}}) Y_{L_4 M_4}(\hat{\mathbf{K}})
\end{aligned}$$

Including the exact form of the mode-coupling, we obtain the reduced angular trispectrum of 21-cm anisotropies due to second-order gravitational perturbation evolution as

$$\begin{aligned}
\mathcal{T}_{\text{grav}}^{l_1 l_2}(L) &= 4 \left(\frac{2}{\pi} \right)^6 \int k_1^d dk_1 \dots \int k_4^d dk_2 \int K^2 dK \int r_1^2 dr_1 \int r_2^2 dr_2 P_\phi(K) P_\phi(k_1) P_\phi(k_3) \sum_{L_1 L_2 L_3 L_4} \tag{44} \\
& \times g_{21\text{cm},l_1}(k_1) g_{21\text{cm},l_2}(k_2) g_{21\text{cm},l_3}(k_3) g_{21\text{cm},l_4}(k_4) j_{l_2}(k_2 r_1) j_{l_4}(k_4 r_2) j_{L_1}(k_1 r_1) j_{L_2}(k_3 r_2) j_{l_3}(K r_1) j_{L_4}(K r_2) \\
& \times \left[\frac{289}{441} S(0,0) + \frac{k_1 k_3}{9K^2} S(1,1) + \frac{136}{2205} S(0,2) + \frac{16}{11025} S(2,2) + \frac{17k_1}{63K} S(1,0) + \frac{17}{63K} S(0,1) + \frac{4k_1}{405K} S(1,2) + \frac{4k_3}{405K} S(2,1) \right],
\end{aligned}$$

where

$$S(l_a, l_b) = \left\{ \begin{matrix} l_1 & l_2 & L \\ L_3 & l_a & L_1 \end{matrix} \right\} \left\{ \begin{matrix} l_3 & l_4 & L \\ L_4 & l_b & L_2 \end{matrix} \right\} h_{L_1 l_1 l_a} h_{L_2 l_3 l_b} h_{L_3 l_2 L_1} h_{L_4 l_4 L_2} h_{L_4 l_b L} h_{L_3 l_a L}, \tag{45}$$

As mentioned above, the angular trispectrum with $T_\delta^{(3)}$ term involves a calculation that is numerically slow given the mode coupling resulting from a term involving $F_3 \propto 1/(k_1+k_2+k_3)^2$ [48]. Since we are considering the 3-1 angular power spectrum, we can ignore the exact momentum dependence of the $\delta^{(3)}$ non-linear gravity and take the angular averaged value of F_3 . The resulting trispectrum in this case takes a simple form similar to that of the primordial trispectrum with a momentum-independent coupling term, and we overestimate the covariance between primordial and non-linear gravity trispectra to the 3-1 angular power spectrum estimator. We do not reproduce the derivation of the angular trispectrum with R_b given that it is similar to equation (23).

-
- [1] S. Furlanetto, S. P. Oh and F. Briggs, arXiv:astro-ph/0608032; X. H. Fan, C. L. Carilli and B. G. Keating, *Ann. Rev. Astron. Astrophys.* **44**, 415 (2006) [arXiv:astro-ph/0602375].
 - [2] G. B. Field, *Astrophys. J.* **129**, 536 (1959); D. Scott and M. J. Rees, *Mon. Not. R. Astr. Soc.* **247**, 510 (1990)
 - [3] A. Loeb and M. Zaldarriaga, *Phys. Rev. Lett.* **92**, 211301 (2004);
 - [4] S. Bharadwaj and S. S. Ali, *Mon. Not. Roy. Astron. Soc.* **352**, 142 (2004).
 - [5] M. Zaldarriaga, S. R. Furlanetto and L. Hernquist, *Astrophys. J.* **608**, 622 (2004).
 - [6] I. T. Iliev, E. Scannapieco, H. Martel and P. R. Shapiro, *Mon. Not. Roy. Astron. Soc.* **341**, 81 (2003).
 - [7] M. G. Santos and A. Cooray, *Phys. Rev. D* **74**, 083517 (2006) [arXiv:astro-ph/0605677],
 - [8] J. D. Bowman, M. F. Morales and J. N. Hewitt, *Astrophys. J.* **661**, 1 (2007) [arXiv:astro-ph/0512262].
 - [9] M. McQuinn, O. Zahn, M. Zaldarriaga, L. Hernquist and S. R. Furlanetto, *Astrophys. J.* **653**, 815 (2006) [arXiv:astro-ph/0512263].
 - [10] U. L. Pen, *New Astron.* **9**, 417 (2004).
 - [11] K. Sigurdson and A. Cooray, *Phys. Rev. Lett.* **95**, 211303 (2005).
 - [12] O. Zahn, A. Lidz, M. McQuinn, S. Dutta, L. Hernquist, M. Zaldarriaga and S. R. Furlanetto, *Astrophys. J.* **654**, 12 (2006) [arXiv:astro-ph/0604177].
 - [13] M. G. Santos, A. Amblard, J. Pritchard, H. Trac, R. Cen and A. Cooray, arXiv:0708.2424 [astro-ph].
 - [14] A. Cooray, *Mon. Not. Roy. Astron. Soc.* **363**, 1049 (2005).
 - [15] S. Bharadwaj and S. K. Pandey, *Mon. Not. Roy. Astron. Soc.* **358**, 968 (2005) [arXiv:astro-ph/0410581].
 - [16] S. Wyithe and M. Morales, arXiv:astro-ph/0703070.

- [17] A. Cooray, Phys. Rev. Lett. **97**, 261301 (2006). arXiv:astro-ph/0610257.
- [18] A. Pillepich, C. Porciani and S. Matarrese, arXiv:astro-ph/0611126.
- [19] E. Komatsu and D. N. Spergel, Phys. Rev. D **63**, 063002 (2001) [arXiv:astro-ph/0005036].
- [20] D. Babich and M. Zaldarriaga, Phys. Rev. D **70**, 083005 (2004) [arXiv:astro-ph/0408455].
- [21] K. M. Smith and M. Zaldarriaga, arXiv:astro-ph/0612571.
- [22] N. Bartolo, E. Komatsu, S. Matarrese and A. Riotto, Phys. Rept. **402**, 103 (2004) [arXiv:astro-ph/0406398].
- [23] R. Scoccimarro, E. Sefusatti and M. Zaldarriaga, Phys. Rev. D **69**, 103513 (2004) [arXiv:astro-ph/0312286].
- [24] N. Dalal, O. Dore, D. Huterer and A. Shirokov, arXiv:0710.4560 [astro-ph].
- [25] J. M. Maldacena, JHEP **0305**, 013 (2003).
- [26] N. Bartolo, S. Matarrese and A. Riotto, Phys. Rev. Lett. **93**, 231301 (2004) [arXiv:astro-ph/0407505].
- [27] E. I. Buchbinder, J. Khoury and B. A. Ovrut, arXiv:0710.5172 [hep-th].
- [28] M. Sasaki, J. Valiviita and D. Wands, Phys. Rev. D **74**, 103003 (2006) [arXiv:astro-ph/0607627].
- [29] D. N. Spergel *et al.*, arXiv:astro-ph/0603449.
- [30] G. D'Amico, N. Bartolo, S. Matarrese and A. Riotto, arXiv:0707.2894 [astro-ph].
- [31] D. Seery, J. E. Lidsey and M. S. Sloth, JCAP **0701**, 027 (2007) [arXiv:astro-ph/0610210].
- [32] N. Kogo and E. Komatsu, Phys. Rev. D **73**, 083007 (2006) [arXiv:astro-ph/0602099].
- [33] L. Boubekeur and D. H. Lyth, Phys. Rev. D **73**, 021301 (2006) [arXiv:astro-ph/0504046].
- [34] A. Cooray, Phys. Rev. D **64**, 043516 (2001).
- [35] G. Chen and I. Szapudi, arXiv:astro-ph/0606394.
- [36] J. N. Fry, Astrophys. J. **297**, 499 (1984).
- [37] M. Liguori, F. K. Hansen, E. Komatsu, S. Matarrese and A. Riotto, Phys. Rev. D **73**, 043505 (2006) [arXiv:astro-ph/0509098].
- [38] M. F. Morales, J. D. Bowman and J. N. Hewitt, arXiv:astro-ph/0510027;
- [39] M. G. Santos, A. Cooray and L. Knox, Astrophys. J. **625**, 575 (2005).
- [40] W. Hu, Phys. Rev. D **64**, 083005 (2001) [arXiv:astro-ph/0105117].
- [41] T. Okamoto and W. Hu, Phys. Rev. D **66**, 063008 (2002) [arXiv:astro-ph/0206155].
- [42] M. A. Riquelme and D. N. Spergel, arXiv:astro-ph/0610007.
- [43] M. H. Goroff, B. Grinstein, S. J. Rey and M. B. Wise, Astrophys. J. **311**, 6 (1986).
- [44] J. N. Fry, Astrophys. J. **279**, 499 (1984).
- [45] R. Scoccimarro, M. Zaldarriaga and L. Hui, Astrophys. J. **527**, 1 (1999) [arXiv:astro-ph/9901099].
- [46] N. Bartolo, S. Matarrese and A. Riotto, JCAP **0508**, 010 (2005) [arXiv:astro-ph/0506410].
- [47] <http://www.lofar.org>; <http://www.haystack.mit.edu/arrays/MWA>
- [48] Analytically, one can still factor out the terms by making use of the Schwinger equality with $(k_1 + k_2 + k_3)^{-2} = \int_0^\infty z e^{-z(k_1+k_2+k_3)} dz$